Magnetic properties of NiMnSb(001) films grown on InGaAs/InP(001)(invited)

B. Heinrich, G. Woltersdorf, R. Urban, and O. Mosendz
Simon Fraser University, 8888 University Dr., Burnaby, BC, V5A 1S6, Canada

G. Schmidt, P. Bach, and L. Molenkamp
Physikalisches Institut (EP3) Universität Würzburg, Am Hubland, 97074 Würzburg, Germany

E. Rozenberg
Physics Department, Ben Gurion University, Beer-Sheva, POB 653 84105, Israel

(Presented on 9 January 2004)

NiMnSb half Heusler alloy films were prepared by molecular beam epitaxy (MBE) on InP(001). The dc and rf magnetic properties were investigated by ferromagnetic resonance (FMR). The effective uniaxial anisotropy fields increased with increasing film thickness and reached nonzero asymptotic values. FMR linewidths rapidly increased with the film thickness due to the presence of two magnon scattering. Bulklike uniaxial anisotropies and two magnon scattering were caused by a self-assembled network of lattice defects. Gilbert damping parameter and spectroscopic g factor were found to be 3.1×10^{7} and 2.03, respectively, indicating a weak role of spin orbit interaction. © *2004 American Institute of Physics.* [DOI: 10.1063/1.1687274]

INTRODUCTION

The progress of semiconductor spintronics depends on the availability of suitable materials. Half metallic ferromagnets meet the demand of high spin polarization at the Fermi level. The NiMnSb half Heusler material is especially attractive due to its high Curie temperature and the possibility to grow it on semiconductor templates. In this work the substrates consist of a semiinsulating InP(001) wafer covered by a 200 nm ($In_{0.53}Ga_{0.47}$ As) buffer layer which is lattice matched to InP. The NiMnSb films investigated in this paper had thicknesses $d=5$, 10, 15, 20, 30, 42, and 85 nm. High resolution x-ray diffraction confirmed very good crystalline quality of the NiMnSb(001) films with the lattice constant $a=5.91\pm0.005$ Å which implies a lattice mismatch to InP(001) of only 0.6%. Further structural details can be found in Ref. 1. Ferromagnetic resonance (FMR) was used to investigate the magnetic properties of the NiMnSb films. The measurements were carried out at 24 and 36 GHz. FMR was measured with the magnetic field applied in the sample plane (parallel configuration), and with the field inclined from the sample plane (out-of-plane configuration).

MAGNETIC ANISOTROPIES

The dependence of the in-plane FMR field on the angle φ between the applied field and the [100] crystallographic axis allows one to determine the in-plane uniaxial anisotropy field $2K_U^{\parallel}/M_s$, fourfold in-plane anisotropy field $2K_1^{\parallel}/M_s$, and effective demagnetizing field $4\pi M_{\mathrm{eff}}=4\pi M_s-2K_U^{\perp}/M_s$. The energy densities $-K_U^{\parallel}(\mathbf{n_U}\cdot\mathbf{m})^2$, $-K_1^{\parallel}/2[\cos^4(\varphi_{\mathbf{m}})+\sin^4(\varphi_{\mathbf{m}})]$ describe explicitly the angular dependence of the in-plane uniaxial and fourfold magnetic anisotropies. **n** and **m** are the unit vectors along the in-plane uniaxial anisotropy axis and the magnetization **M**, respectively. $\varphi_{\mathbf{m}}$ is the angle between **m** and the [100] direction. $K_U^{\perp}$ is the effective perpendicular uniaxial anisotropy and M_s is the saturation magnetization. $2K_U^{\parallel}/M_s$ as a function of the film thickness is shown in Fig. 1. The perceived asymptotic value ($d\to\infty$) of $2K_U^{\parallel}/M_s$ is -200 Oe with the hard axis along the $[1\bar{1}0]$ direction of the InP(001) wafer. The uniaxial anisotropy in the thick films arises most likely from an in-plane anisotropic strain.[2] A well defined $1/d$ dependence for the samples thinner than 15 nm indicates that the NiMnSb films possess an in-plane uniaxial interface anisotropy, $K_{Us}^{\parallel}=0.08$ erg/cm^2. Its origin is most likely associated with the interface chemistry between NiMnSb(001) and InGaAs(001). The fourfold in-plane and perpendicular uniaxial fields as a function of the

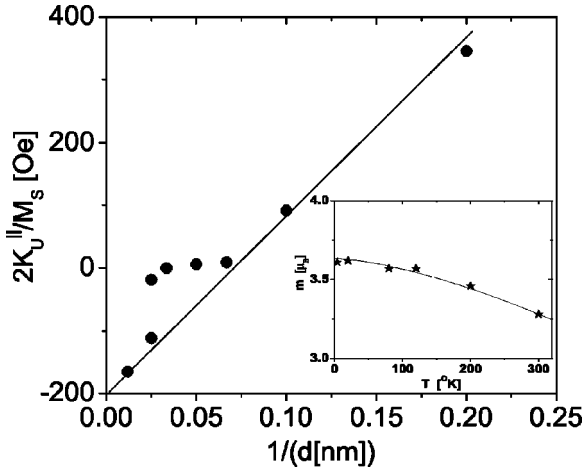

FIG. 1. The in-plane uniaxial anisotropy field, $2K_U^{\parallel}/M_s$ as a function of $1/d$, where d is the NiMnSb(001) film thickness. Note that the films in the intermediate thickness range have nearly zero uniaxial anisotropy. The in-plane uniaxial anisotropy axis is along the $[1\bar{1}0]$ direction with respect to the InP(001) template. The inset shows the temperature dependence of the magnetic moment per NiMnSb formula unit in Bohr magnetons for the 42 nm thick film. The solid line represents a $T^{3/2}$ fit. A good fit to the data indicates that thermal excitations of three-dimensional spin waves are responsible for the decrease of the magnetic moment with an increasing temperature T.

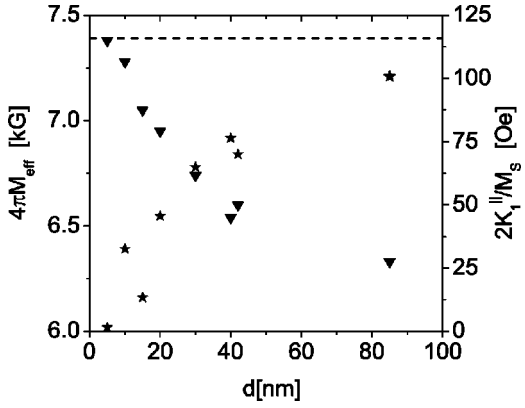

FIG. 2. The in-plane fourfold anisotropy field $2K_1^{\parallel}/M_s$ ($\star$) and the effective demagnetizing field $4\pi M_{\text{eff}}$ ($\blacktriangledown$) as function of d. The dashed vertical line indicates the value of $4\pi M_s$ determined by SQUID magnetometery in Fig. 1. Note that with increasing film thickness the uniaxial field $2K_U^{\perp}/M_s$ acquires bulklike character due to lattice strain.

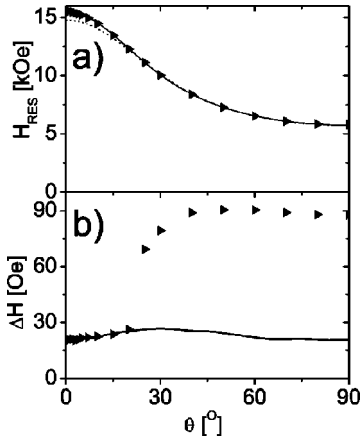

FIG. 3. (a) The dependence of the FMR field for the out of plane FMR measurements at 24 GHz on a 42 nm thick sample. The applied dc field is held in (110) plane. $\theta=90°$ correspond to the in-plane FMR (the magnetic moment along the [110] direction); $\theta=0$ corresponds to the perpendicular FMR with the magnetization along the [001] direction. The dotted line represents the calculated dependence of the FMR field using $2K_1^{\perp}/M_s = 2K_1^{\parallel}/M_s = 77$ Oe, $g=2.05$, $4\pi M_{\text{eff}}=6.5$ kG. The best fit (solid line) breaks the in-plane/out-of-plane symmetry and required $2K_1^{\perp}/M_s=-517$ Oe, $g=2.03$, and $4\pi M_{\text{eff}}=6.65$ kG. (b) The angular dependence of the FMR linewidth. The solid line represents the calculated angular dependence of the intrinsic damping, $G=3.1\times10^7$ Hz. The difference between the data and solid line shows the effectiveness of two magnon scattering as a function of the angle θ. Note the perfect agreement between the calculation and the data for $\theta<20°$.

film thickness were not well described by constant (bulklike) and $1/d$ (interface) contributions. Superconducting quantum interference device (SQUID) magnetometery (quantum design) was used to determine the magnetic moment of the 42 nm sample, see inset of Fig. 2. The thickness of this sample was determined by an x-ray interference technique. The magnetic moment was found to be $(3.3\pm0.1)\mu_B$ and $(3.6\pm0.1)\mu_B$ per NiMnSb formula unit at 300 K and 4 K, respectively. The theoretical magnetic moment is expected to be $\mu_B=4.0$ (Ref. 3) and was observed in bulk samples.[4] The lower value of the magnetic moment observed in our films is most likely caused by growth induced lattice defects, see below and Ref. 5. The perpendicular uniaxial field increases with increasing film thickness, see Fig. 2, asymptotically approaching constant value of ~1.1 kOe indicating bulklike tetragonal distortions due to the lattice strain. The out-of-plane dependence of the FMR field on the angle θ allows one to determine the fourfold perpendicular anisotropy field $2K_1^{\perp}/M_s$ and the gyromagnetic ratio γ with its corresponding g factor. θ is the angle between the applied magnetic field and the sample normal. $-K_1^{\perp}\cos^4(\theta_{\mathbf{m}})$ describes the angular dependence of the fourfold perpendicular anisotropy. The dotted line in Fig. 3(a) shows that a perfect cubic symmetry ($K_1^{\perp}=K_1^{\parallel}$) does not represent the data well when the magnetization is inclined under a large angle with respect to the film surface. The best fit is obtained by using $2K_1^{\perp}/M_s=-517$ and -295 Oe for the 42 and 15 nm thick films, respectively. Note, that even the sign of $2K_1^{\perp}/M_s$ is different from the corresponding in-plane field $2K_1^{\parallel}/M_s$. Obviously, the films have built in increasing tetragonal lattice distortion with increasing film thickness. The g factor was found to be 2.03 and 2.02 for the 42 and 15 nm thick films, respectively. The parameter $\Delta g=g-2\sim0.02$ is very small indicating weak spin orbit interaction.

MAGNETIC DAMPING

Significant information can be obtained by investigating the FMR linewidth, ΔH. The angular dependence of ΔH is shown in Fig. 4. One can identify angular independent ΔH_0, fourfold $\Delta H_4\cos^2(2\varphi_{\mathbf{m}})$, and twofold $\Delta H_2\cos^2(\varphi_{\mathbf{m}})$ contributions. ΔH increased rapidly with increasing film thickness, see Fig. 4. For the thinnest sample ($d=5$ nm), the lowest value of the FMR linewidth was 20 Oe at 24 GHz along the $\langle100\rangle$ crystallographic directions. This FMR linewidth scaled linearly with the microwave frequency with no zero frequency offset. Therefore, the magnetic damping with the magnetization along $\langle100\rangle$ is caused by Gilbert damping. The Gilbert damping parameter has a remarkably low value, $G=3.1\times10^7$ s^{-1}. The smallest Gilbert damping in the $3d$ transition element metals was observed for bcc Fe, $G=6\times10^7$ s^{-1} (Ref. 6). The Gilbert damping parameter in NiMnSb is even appreciably smaller than that in Fe. In metallic samples the Gilbert damping parameter is caused by spin orbit interaction.[7] The small deviation of the g factor

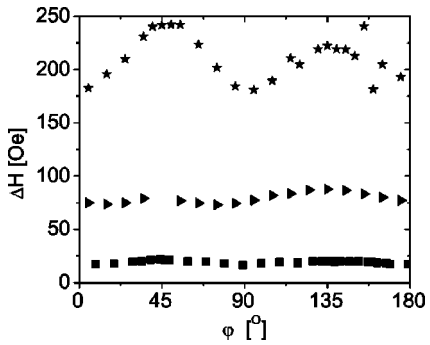

FIG. 4. The FMR linewidth as a function of the angle $\varphi_{\mathbf{m}}$ between the magnetization and the in-plane crystalline [100] axis. The measurements were carried out at 24 GHz. (■), (▶), and ($\star$) correspond to the thickness 5, 42, and 85 nm, respectively. Note a pronounced angular dependence.

from 2 and the small Gilbert damping consistently indicate that the role of spin orbit interaction is rather weak in NiMnSb.

Out-of-plane FMR measurements on the 15, 42, and 85 nm thick films strongly suggest that a rapid increase of ΔH with an increasing film thickness (see Fig. 4) is caused by lattice defects. The FMR linewidth with the direction of the magnetic moment close to the film normal decreased rapidly to the value that corresponds to the intrinsic Gilbert damping, see Fig. 3(b). This behavior is a hallmark of two magnon scattering.[8] In the perpendicular configuration no magnons have the precessional frequency equal to that of the FMR mode (applied microwave angular frequency ω), and consequently two magnon scattering is absent. It follows that the additional FMR line broadening in the NiMnSb films is caused by two magnon scattering relaxation.

Work by Heinrich's group at Simon Fraser University (SFU) (Refs. 9–11) has shown that lattice defects in crystalline epitaxial structures can result in extrinsic damping which has an appreciable angular dependence. In our recent studies of Pd/Fe/GaAs(001) structures we found[11] that a rectangular network of misfit dislocations leads to a large angular dependent two magnon scattering. The FMR linewidth reached a maximum with the magnetization oriented along the lines of misfit dislocations and was very weak at 45° away from these lines. A similar behavior in ΔH was found in the NiMnSb films discussed in this paper.

Plan view TEM studies on the NiMnSb films carried out by Kavanagh's group at SFU fully support this picture. The TEM studies have shown that in the NiMnSb films the lattice defects consist of two rectangular networks of lattice defects with defect lines parallel to the $\langle 100 \rangle$ and $\langle 110 \rangle$ in-plane crystallographic axes.[5] The measured angular dependence of the FMR linewidth, see Figs. 3 and 4, allows one to draw several conclusions.

(i) Figure 3(b) shows that the effectiveness of the two magnon scattering mechanism is very weakly dependent on the angle of the magnetic moment with respect to the sample surface until the magnetization is close to the film normal where it rapidly collapses to zero. This was found to be a common feature of two magnon scattering in recently studied systems.[8,11]

(ii) A large angle independent contribution ΔH_0 indicates that thick NiMnSb films are affected by a sizeable isotropic in-plane lattice disorder.

(iii) A noticeable $\Delta H_2 \cos^2(\varphi_{\mathbf{m}})$ indicates that the distribution of lattice defects is not equivalent along two mutually perpendicular crystalline axes, e.g., $\langle 100 \rangle$ and $\langle 010 \rangle$. This means the network of defect lines does not satisfy fully the square symmetry of the (001) template. This is in accord with the increasing in-plane uniaxial anisotropy $K_U^{\parallel}$ with increasing film thickness.

The presence of crystallographic defects also strongly affects the width of hysteresis loops. With an increasing defect density the coercive field increased from 3 Oe to 60 Oe.

SUMMARY

The FMR measurements have shown that the NiMnSb films grown by MBE on InP(001) wafers are accompanied by defects with a decreased lattice symmetry. A self-assembled network of lattice defects increases its prominence with an increasing film thickness. Consequently it is hard to identify the intrinsic properties of NiMnSb corresponding to a perfect cubic lattice. The g factor is very close to the free electron value and the intrinsic damping is the smallest among all known ferromagnetic metals indicating that the role of spin orbit interaction is weak in NiMnSb. A self-assembled defect network generates a strong two magnon scattering which can surpass significantly the intrinsic Gilbert damping. The two magnon scattering has a pronounced angular dependence which reflects the angular symmetry of the magnetic defect scattering in the reciprocal space.[11] In our view the presence of angular dependent damping is in general a ''smoking gun'' indicating the presence of extrinsic damping.

ACKNOWLEDGMENTS

The authors acknowledge the financial support from the Natural Sciences and Engineering Research Council of Canada (NSERC) and Canadian Institute for Advanced Research (CIAR). G.W. thanks the German Academic Exchange Service (DAAD) for a generous scholarship.

[1] P. Bach *et al.*, Appl. Phys. Lett. **83**, 521 (2003).
[2] O. Thomas, Q. Schen, O. Schieffer, and P. Lepine, Phys. Rev. Lett. **90**, 017205 (2003).
[3] R. de Groot, F. Mueller, P. van Engen, and K. Bushow, Phys. Rev. Lett. **50**, 2024 (1983).
[4] l. Ritchie *et al.*, Phys. Rev. B **68**, 104430 (2003).
[5] A. Kooeshnikoo, G. Woltersdorf, J. Q. Lin, A. Moseudz, E. Rosenberg, B. Heinrich, K. L. Kavaugh, P. Bach, A. S. Bader, C. Rüster, G. Gould, G. Schmidt, and L. W. Molenkaup, J. Vac. Sci. Technol. A (to be published).
[6] Z. Frait and D. Fraitova, J. Magn. Magn. Mater. **15–18**, 1081 (1980).
[7] B. Heinrich, R. Urban, and G. Woltersdorf, J. Appl. Phys. **91**, 7523 (2002).
[8] R. Urban, B. Heinrich, G. Woltersdorf, K. Ajdari, K. Myrtle, J. Cochran, and E. Rozenberg, Phys. Rev. B **65**, 020402 (2002).
[9] B. Heinrich, S. Purcell, J. Dutcher, K. Urquhart, J. Cochran, and A. Arrott, Phys. Rev. B **38**, 12 879 (1988).
[10] Z. Celinski and B. Heinrich, J. Appl. Phys. **70**, 5935 (1991).
[11] G. Woltersdorf and B. Heinrich (unpublished).